nature immunology

Apoptosis in response to microbial infection induces autoreactive T_H17 cells

Laura Campisi[7], Gaetan Barbet[1,2], Yi Ding[3], Enric Esplugues[4], Richard A Flavell[4] & J Magarian Blander[1,2,5,6]

Microbial infections often precede the onset of autoimmunity. How infections trigger autoimmunity remains poorly understood. We investigated the possibility that infection might create conditions that allow the stimulatory presentation of self peptides themselves and that this might suffice to elicit autoreactive T cell responses that lead to autoimmunity. Self-reactive CD4$^+$ T cells are major drivers of autoimmune disease, but their activation is normally prevented through regulatory mechanisms that limit the immunostimulatory presentation of self antigens. Here we found that the apoptosis of infected host cells enabled the presentation of self antigens by major histocompatibility complex class II molecules in an inflammatory context. This was sufficient for the generation of an autoreactive T_H17 subset of helper T cells, prominently associated with autoimmune disease. Once induced, the self-reactive T_H17 cells promoted auto-inflammation and autoantibody generation. Our findings have implications for how infections precipitate autoimmunity.

Autoimmunity is caused by pathogenic T cell and B cell responses directed against self[1–4]. Genetic background is the strongest predisposing factor for autoimmunity; however, studies reporting disease discordance in identical twins and the large heterogeneity within a single disease[2,5] indicate an additional role for environmental factors. Epidemiological studies have linked microbial infection and autoimmunity, which suggests that infection can trigger autoimmune disease[6–9]. Several theories have been proposed, including the bystander activation of autoreactive T cells by inflammation or pathogen-encoded super-antigens, as well as 'epitope mimicry', whereby self-reactive T cells are activated inappropriately by microbial peptides with homology to those from self[6,10]. Whether the response of innate immune cells to infection induces the activation of self-reactive adaptive responses is not known. Instead of invoking 'epitope mimicry', we investigated whether the presentation of self peptides themselves might be possible during certain infections and might result in the activation and subsequent differentiation of self-reactive T cells.

The presentation of self peptides by dendritic cells (DCs) in the context of inflammation and T cell co-stimulation is normally avoided and is thought to represent one mechanism of peripheral tolerance that prevents the priming of self-reactive T cells[11]. *In vitro* studies have shown that antigen presentation by bone-marrow-derived DCs (BMDCs) is regulated by Toll-like receptor (TLR) signals specifically from phagosomes containing pathogens and not from those containing apoptotic cells. This subcellular mechanism favors the presentation of microbial antigens over that of cellular antigens by major histocompatibility complex (MHC) class I and class II molecules[11,12]. However, the phagocytosis of infected apoptotic cells delivers into the same phagosome both cellular antigens and microbial antigens, along with TLR ligands. Whether MHC class II molecules present self antigens and non-self antigens in this scenario has never been investigated.

Here we found that during an infection that causes the apoptosis of infected colonic epithelial cells, self-reactive CD4$^+$ T cells with specificity to cellular antigens were activated along with CD4$^+$ T cells specific to the infecting pathogen. The self-reactive CD4$^+$ T cells differentiated into T_H17 cells, concordant with the inflammatory environment elicited by the combination of infection and apoptosis, which favors the development of a T_H17 response[13,14]. We found that the emergence of self-reactive T_H17 cells during colonic infection was associated with autoantibody production, along with enhanced susceptibility to intestinal inflammation. Our results have implications for understanding how microbial infection can elicit a break in tolerance and set the stage for the subsequent development of autoimmunity.

RESULTS

MHC class II presentation of infected-apoptotic-cell antigen

Cellular antigens from apoptotic cells were presented by BMDCs only when those apoptotic cells concurrently contained a TLR ligand[11,12] (**Supplementary Fig. 1a**). Because the phagocytosis of infected apoptotic cells would deliver TLR ligands along with cellular and microbial antigens to the same phagosome, we sought to determine whether cellular antigen could be presented alongside microbial antigen in this scenario. We infected mouse A20 lymphoma B cells that express the

[1]Immunology Institute, Icahn School of Medicine at Mount Sinai, New York, New York, USA. [2]Department of Medicine, Icahn School of Medicine at Mount Sinai, New York, New York, USA. [3]Department of Pathology, New York University Langone Medical Center, New York, New York, USA. [4]Department of Immunobiology, Yale University School of Medicine, New Haven, Connecticut, USA. [5]Tisch Cancer Institute, Icahn School of Medicine at Mount Sinai, New York, New York, USA. [6]Department of Microbiology, Icahn School of Medicine at Mount Sinai, New York, New York, USA. [7]Present addresses: Department of Microbiology, Icahn School of Medicine at Mount Sinai, New York, New York, USA, and Global Health and Emerging Pathogens Institute, Icahn School of Medicine at Mount Sinai, New York, New York, USA. Correspondence should be addressed to J.M.B. (julie.blander@mssm.edu).

Received 24 March; accepted 9 June; published online 25 July 2016; doi:10.1038/ni.3512

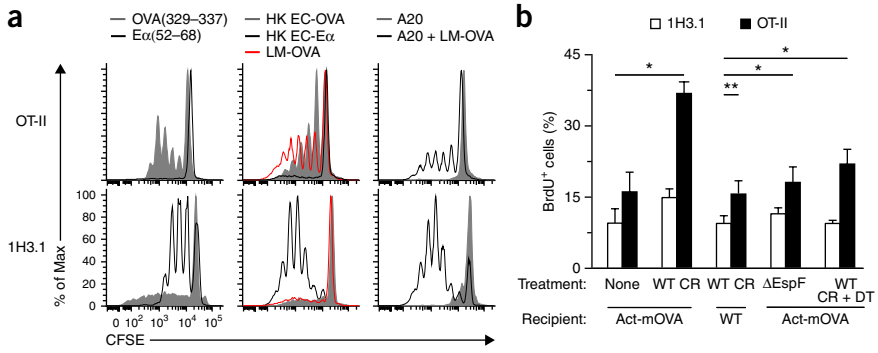

Figure 1 Presentation of apoptotic-cell-derived antigens during infection. (**a**) Proliferation of OT-II and 1H3.1 CD4$^+$ T cells (left margin) in response to BMDCs pulsed with OVA(329–337) or Eα(52–69) (left), phagocytosis of recombinant heat-killed *E. coli* expressing OVA (HK EC-OVA) or Eα (HK EC-Eα) or LM-OVA (middle), or phagocytosis of uninfected Eα$^+$ A20 cells (A20) or LM-OVA-infected apoptotic Eα$^+$ A20 cells (A20 + LM-OVA) (right), presented as dilution of the division-tracking dye CFSE. (**b**) Frequency of proliferating (BrdU$^+$) LI LP cells in Act-mOVA host mice given CD11c-DTR bone marrow and OT-II T cells plus 1H3.1 T cells and left uninfected (None) ($n = 6$) or infected with wild-type *C. rodentium* (WT CR) ($n = 7$), in wild-type host mice given bone marrow and T cells as above and infected with wild-type *C. rodentium* ($n = 6$), or in Act-mOVA host mice given bone marrow and T cells as above and infected with ΔEspF *C. rodentium* ($n = 9$) or infected with wild-type *C. rodentium* and treated with diphtheria toxin (WT CR+DT) ($n = 6$), assessed by flow cytometry with gating on $V_\beta6^+$ (1H3.1) CD4$^+$ T cells or $V_\alpha2^{hi}V_\beta5^+$ (OT-II) CD4$^+$ T cells. $^*P \le 0.01$ and $^{**}P \le 0.001$ (one-way analysis of variance (ANOVA) and Tukey's post-test). Data are representative of three experiments (mean + s.d. in **b**).

α-chain of I-E (Eα antigen) with recombinant *Listeria monocytogenes* expressing ovalbumin (LM-OVA), followed by induction of apoptosis with recombinant Fas ligand. Phagocytosis of LM-OVA–infected apoptotic A20 cells by BMDCs derived from C57BL/6J mice, which do not express Eα, led to the proliferation of both 1H3.1 CD4$^+$ T cells (with transgenic expression of an Eα-specific T cell antigen receptor (TCR)) and OT-II CD4$^+$ T cells (with transgenic expression of an OVA-specific TCR), but similar phagocytosis of uninfected A20 cells did not (**Fig. 1a** and **Supplementary Fig. 1b**). As expected, T cells proliferated in response to their respective cognate antigens derived from LM-OVA or from recombinant *E. coli* expressing OVA or Eα or to specific peptide pulsed onto BMDCs (**Fig. 1a**).

We next turned to orogastric infection with the rodent pathogen *Citrobacter rodentium*, which infects colonic intestinal epithelial cells and induces their apoptosis[13]. We generated chimeric mice by reconstituting lethally irradiated Act-mOVA mice (which have transgenic expression of a membrane-bound form of OVA (mOVA) under control of the promoter of the ubiquitous gene encoding β-actin) with bone marrow from donor CD11c-DTR mice (which express the diphtheria toxin receptor (DTR) under control of the promoter of the gene encoding the integrin CD11c and are transiently depleted of DC populations after treatment with diphtheria toxin) (**Supplementary Fig. 1c**). As a control, we generated chimeric mice in which wild-type C57BL/6J mice served as recipients (**Supplementary Fig. 1c**). We adoptively transferred OT-II T cells ($V_\alpha2^+V_\beta5^+$), specific to the self-antigen OVA in this model, together with 1H3.1 T cells ($V_\beta6^+$), for which no cognate antigen is present, into the chimeric host mice. After infection of the host mice with *C. rodentium*, the transferred OT-II T cells proliferated more in Act-mOVA chimeras than in wild-type chimeras, and this proliferation was driven by OVA, as no such proliferation of 1H3.1 T cells was induced by infection (**Fig. 1b**). Both populations of T cells proliferated to a limited extent after transfer regardless of the presence or absence of cognate antigens and to an extent similar to that in uninfected mice (**Fig. 1b**). OT-II T cells no longer proliferated in response to infection after diphtheria-toxin-induced depletion of CD11c$^+$ cells or in response to infection with ΔEspF *C. rodentium*, a variant that lacks the secreted protein EPEC that mediates apoptosis[13] (**Fig. 1b**). As expected, 1H3.1 T cells did not proliferate in response to either of those conditions (**Fig. 1b**) but did proliferate after injection of wild-type C57BL/6J mice with Eα-expressing *E. coli* (**Supplementary Fig. 1d**). These data indicated that cellular antigens were presented by CD11c$^+$ cells during infection with *C. rodentium* and were presented in a manner dependent on the ability of infecting bacteria to induce apoptosis.

Pathogen-specific CD4$^+$ T cells induced by *C. rodentium* infection

Intestinal T_H17 responses are typically measured by antigen-nonspecific stimulation *ex vivo* with the phorbol ester PMA and ionomycin (**Fig. 2a** and **Supplementary Fig. 2a**). To assess the antigen specificity of the T_H17 CD4$^+$ T cell response in mice following infection with *C. rodentium*, we stimulated CD4$^+$ T cells from the mesenteric lymph nodes (MLNs) or large intestinal lamina propria (LI LP) with splenocytes pulsed with lysates of *C. rodentium* or the control pathogen *Listeria monocytogenes*. A much smaller proportion of CD4$^+$ T cells from infected mice responded by producing more interleukin 17 (IL-17) in response to *C. rodentium* than in response to *L. monocytogenes*, relative to the proportion of such cells obtained by stimulation with PMA and ionomycin (**Fig. 2a** and **Supplementary Fig. 2a**). A fraction of *C. rodentium*–specific LI LP IL-17$^+$ CD4$^+$ T cells also produced interferon-γ (IFN-γ) and IL-22 (**Supplementary Fig. 2a**). IL-17$^+$CD4$^+$ T cells expressed the T_H17 cell–specific transcription factor RORγt (**Fig. 2b**) and had low expression of the T_H1 cell–specific transcription factor T-bet but not of the regulatory T cell (T_{reg} cell)–specific transcription factor Foxp3 (**Supplementary Fig. 2a**,**b**), consistent with published reports[15]. MLN CD4$^+$ T cells from infected mice secreted IL-17, IFN-γ and IL-22 when re-stimulated *ex vivo* with lysates of *C. rodentium* but not when re-stimulated *ex vivo* with lysates of *L. monocytogenes* (**Fig. 2c**). Consistent with published studies[16], colonic T_H17 cells did not produce the IL-10 characteristic of regulatory T_H17 cells in the small intestine[17,18] (**Supplementary Fig. 2c**). Instead, we noted less production of IL-10 by CD4$^+$ T cells from infected mice than by those from uninfected mice, and this IL-10 production was confined to Foxp3$^+$ T_{reg} cells (**Supplementary Fig. 2c**).

Consistent with the fact that the T_H17 immune response is contingent on infection-induced apoptosis of colonic epithelial cells[13,14], the production of IL-17 by *C. rodentium*–specific LI LP CD4$^+$ T cells was impaired after infection with ΔEspF *C. rodentium* relative to its production after infection with wild-type *C. rodentium* (**Fig. 2d**,**e**), despite the similar proliferation of T cells in response to infection with wild-type *C. rodentium* or ΔEspF *C. rodentium* (**Fig. 2d**). Indeed, 50–60% of LI LP CD4$^+$ T cells proliferated in response to infection with either wild-type *C. rodentium* or ΔEspF *C. rodentium*, compared with an average of 20% in uninfected mice (**Fig. 2d**), reflective of

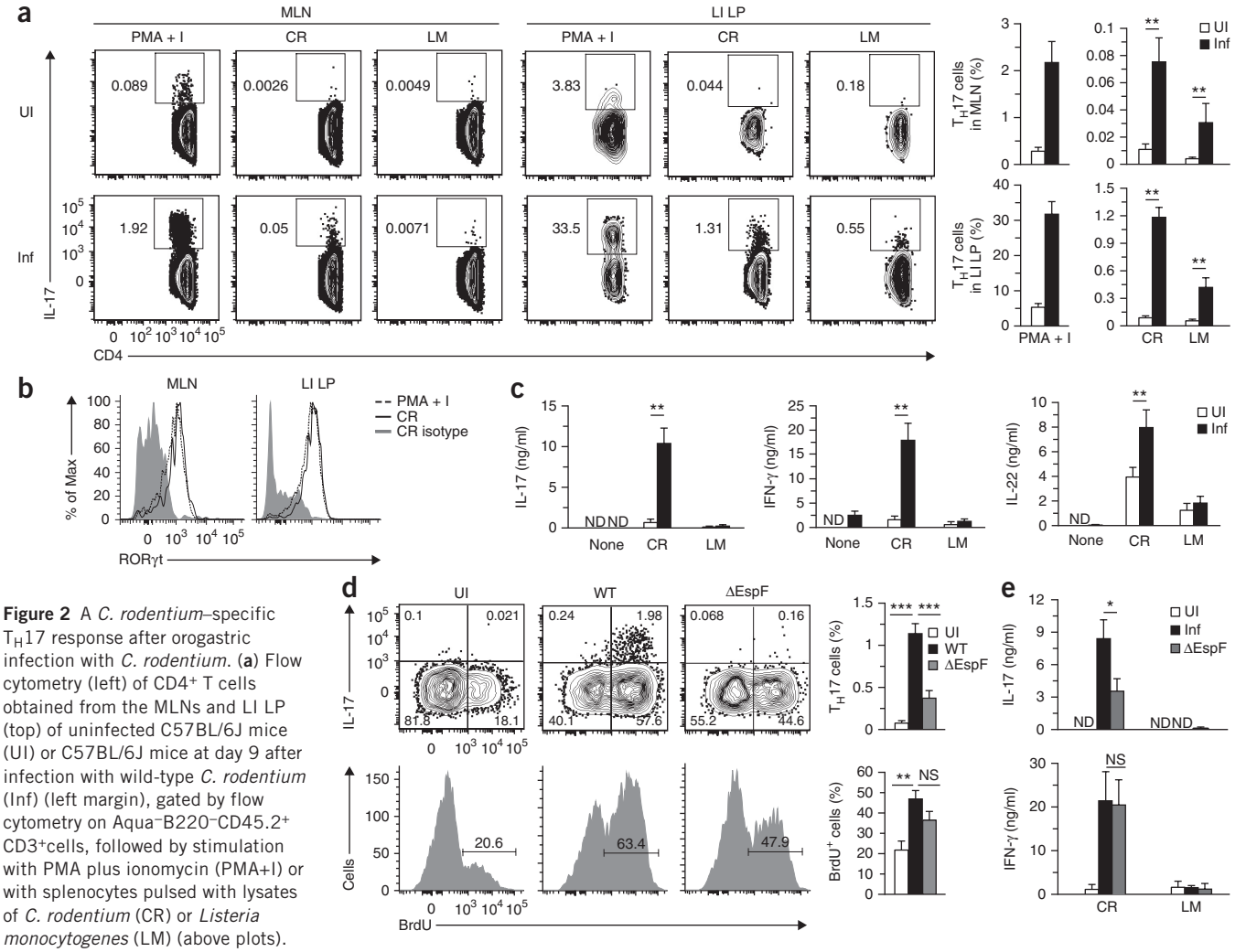

Figure 2 A *C. rodentium*–specific T_H17 response after orogastric infection with *C. rodentium*. (**a**) Flow cytometry (left) of CD4$^+$ T cells obtained from the MLNs and LI LP (top) of uninfected C57BL/6J mice (UI) or C57BL/6J mice at day 9 after infection with wild-type *C. rodentium* (Inf) (left margin), gated by flow cytometry on Aqua$^-$B220$^-$CD45.2$^+$ CD3$^+$cells, followed by stimulation with PMA plus ionomycin (PMA+I) or with splenocytes pulsed with lysates of *C. rodentium* (CR) or *Listeria monocytogenes* (LM) (above plots). Numbers adjacent to outlined areas indicate percent IL-17$^+$CD4$^+$ (T_H17) cells. Right, quantification of results at left ($n = 9$ mice). (**b**) RORγt expression by IL-17$^+$CD4$^+$ T cells obtained from the MLNs or LI LP of mice ($n = 5$) infected and treated as in **a** (key), assessed by flow cytometry. (**c**) ELISA of IL-17, IFN-γ and IL-22 in supernatants of CD4$^+$ T cells obtained from the MLNs of uninfected mice or mice infected with wild-type *C. rodentium* ($n = 12$) and left unstimulated (None) or re-stimulated *ex vivo* with pathogen-pulsed splenocytes as in **a** (horizontal axes). (**d**) Flow cytometry (left) analyzing the IL-17 production (top) and proliferation (bottom) of CD4$^+$ T cells (gated as in **a**) from the LI LP of C57BL/6J mice left uninfected or at day 9 after infection with wild-type or ΔEspF *C. rodentium* (key). Numbers in quadrants (top) indicate percent cells in each (throughout); numbers above bracketed lines (bottom) indicate percent BrdU$^+$ (proliferated) cells. Right, quantification of the results at left, for uninfected mice ($n = 7$) or mice infected with wild-type *C. rodentium* ($n = 9$) or ΔEspF *C. rodentium* ($n = 8$). (**e**) ELISA of IL-17 and IFN-γ in supernatants of CD4$^+$ T cells obtained from the MLNs of mice left uninfected ($n = 9$) or infected with wild-type *C. rodentium* ($n = 9$) or ΔEspF *C. rodentium* ($n = 9$ (IL-17) or $n = 12$ (IFN-γ)) (key) and re-stimulated *ex vivo* with pathogen-pulsed splenocytes as in **a** (horizontal axes). ND, not detected. NS, not significant ($P > 0.05$); $^*P \le 0.05$, $^{**}P \le 0.01$ and $^{***}P \le 0.001$ (one-way ANOVA and Dunnett's post-test (**a**), one-way ANOVA and Tukey's post-test (**d**) or Mann-Whitney test (**c**,**e**)). Data are representative of three independent experiments (**a**,**d**; mean + s.d.), two independent experiments (**b**) or four experiments (**c**,**e**; mean + s.d.).

homeostatic T cell proliferation in response to the gut microbiota[19]. We also noted similar shortening of the colon in response to infection with wild-type *C. rodentium* or ΔEspF *C. rodentium* and similar fecal and colonic abundance of these bacteria (**Supplementary Fig. 2d**), as reported before[13]. Finally, after re-stimulation *ex vivo* with bacterial-lysate-pulsed splenocytes, IL-17 production by CD4$^+$ T cells was impaired in mice infected with ΔEspF *C. rodentium* relative to its production in mice infected with wild-type *C. rodentium*, but the secretion of IFN-γ was similar in these conditions (**Fig. 2e**). Accordingly, LI LP CD4$^+$ T cells had similar expression of T-bet after infection with either bacterial strain, while RORγt was expressed specifically after infection with wild-type *C. rodentium* but not after infection with ΔEspF *C. rodentium* (**Supplementary Fig. 2e**). Consistent with published findings[20], the frequency of Foxp3$^+$ cells was diminished after infection with either wild-type *C. rodentium* or ΔEspF *C. rodentium* (**Supplementary Fig. 2a**,**e**). Therefore, a lack of apoptosis during infection did not affect the priming of CD4$^+$ T cells in response to *C. rodentium* antigens but instead impaired the differentiation of *C. rodentium*–specific T_H17 cells.

Tracking self-reactive and pathogen-specific CD4$^+$ T cells

T_H17 cells mobilized after infections that cause apoptosis might be specific not only to the infecting pathogen but also to self antigen from infected apoptotic cells. Unlike endogenous autoreactive T cells, adoptively transferred T cells specific to a self antigen in recipient mice (**Fig. 1b**) would not undergo central tolerance. To investigate whether the apoptosis of infected cells could activate endogenous self-reactive T cells, we resorted to an experimental model typically used for the enrichment

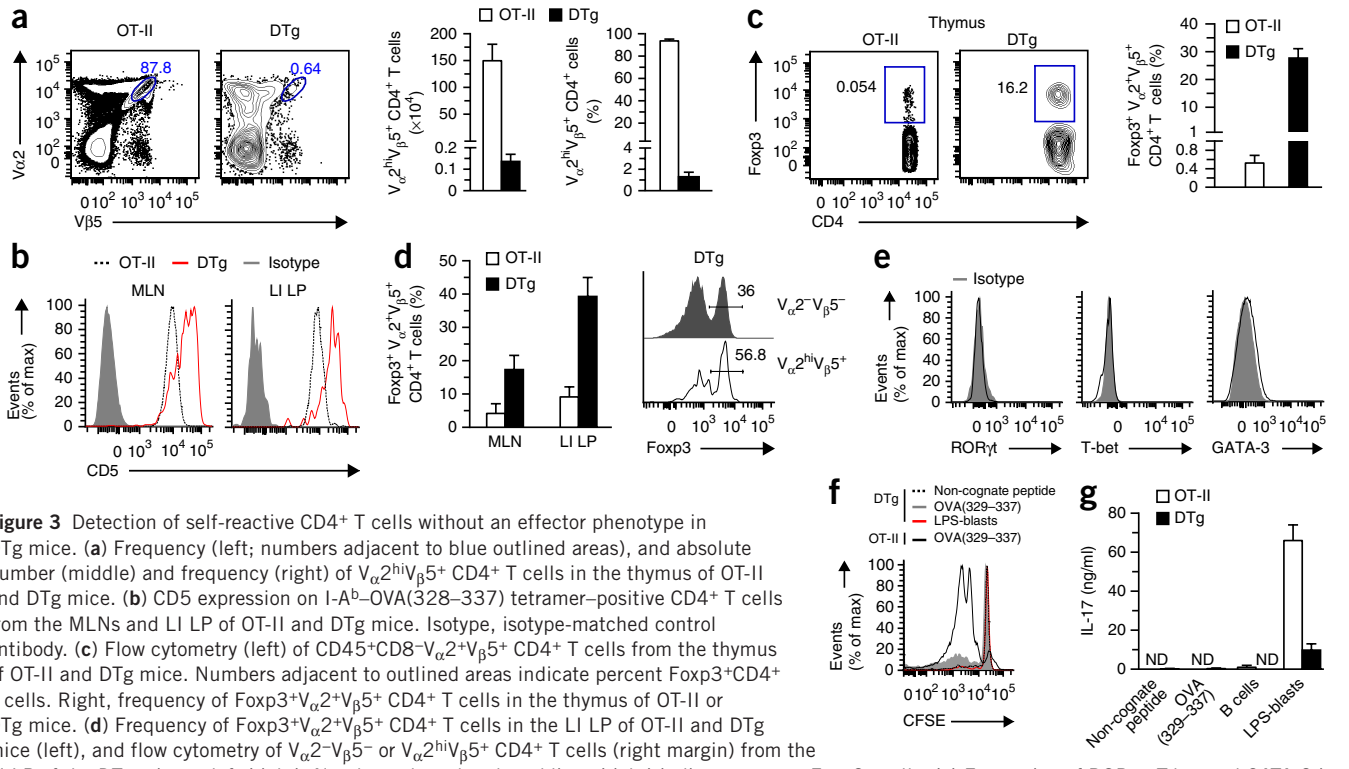

Figure 3 Detection of self-reactive CD4$^+$ T cells without an effector phenotype in DTg mice. (**a**) Frequency (left; numbers adjacent to blue outlined areas), and absolute number (middle) and frequency (right) of $V_\alpha2^{hi}V_\beta5^+$ CD4$^+$ T cells in the thymus of OT-II and DTg mice. (**b**) CD5 expression on I-A^b–OVA(328–337) tetramer–positive CD4$^+$ T cells from the MLNs and LI LP of OT-II and DTg mice. Isotype, isotype-matched control antibody. (**c**) Flow cytometry (left) of CD45$^+$CD8$^-$$V_\alpha2^+V_\beta5^+$ CD4$^+$ T cells from the thymus of OT-II and DTg mice. Numbers adjacent to outlined areas indicate percent Foxp3$^+$CD4$^+$ T cells. Right, frequency of Foxp3$^+$$V_\alpha2^+V_\beta5^+$ CD4$^+$ T cells in the thymus of OT-II or DTg mice. (**d**) Frequency of Foxp3$^+$$V_\alpha2^+V_\beta5^+$ CD4$^+$ T cells in the LI LP of OT-II and DTg mice (left), and flow cytometry of $V_\alpha2^-V_\beta5^-$ or $V_\alpha2^{hi}V_\beta5^+$ CD4$^+$ T cells (right margin) from the LI LP of the DTg mice at left (right). Numbers above bracketed lines (right) indicate percent Foxp3$^+$ cells. (**e**) Expression of RORγt, T-bet and GATA-3 in $V_\alpha2^{hi}V_\beta5^+$ LI LP CD4$^+$ T cells from uninfected DTg mice, assessed by flow cytometry. (**f**) Proliferation (CFSE dilution) of splenic CD25$^-$CD4$^+$ T cells from OT-II or DTg mice (key) after 5 d of culture with BMDCs pulsed with non-cognate peptide or OVA(329–337) (each at 10 μg/ml) or with BMDCs that had phagocytosed LPS-stimulated (LPS-blasts) apoptotic B cells isolated from Act-mOVA BALB/c mice. (**g**) Secretion of IL-17 by splenic T cells as in **f**, as well as T cells stimulated with BMDCs that had phagocytosed unstimulated apoptotic B cells from Act-mOVA BALB/c mice (B cells), assessed after 48 h of secondary re-stimulation with OVA(329–337). Data are representative of two independent experiments (**a**–**c**, **d**, right, **e**–**g**; mean + s.d. in **a**,**c**,**d**,**g**) with $n = 5$ (**a**–**c** and **d**, right) or $n = 4$ (**e**) mice, or three independent experiments with $n = 9$ mice (**d**, left; mean + s.d.).

of natural T_{reg} cells in which mice have transgenic expression of a TCR as well as its high-affinity cognate antigen[21–23]. For this, we crossed OT-II mice with Act-mOVA mice (**Supplementary Fig. 3a**). The resultant offspring (called 'double-transgenic' (DTg) mice here) had OT-II CD4$^+$ T cells specific to OVA as a self antigen. Consistent with published studies[21–23], OVA-specific T cells in DTg mice underwent massive deletion but were still detectable in the thymus (at an abundance of ~1%, compared with an abundance of ~95% in OT-II mice) (**Fig. 3a**), as well as in the MLNs (~5%) and large intestine (~8–10%), where a major polyclonal CD4$^+$ T cell population was also present (**Supplementary Fig. 3b**,**c**), reflective of pairing of the transgenically expressed TCRβ chain with endogenous TCRα chains[24]. We detected OT-II CD4$^+$ T cells in the secondary lymphoid organs of DTg mice on the basis of high expression of α-chain variable region 2 ($V_\alpha2$), to exclude the detection of T cells expressing endogenous TCRα chains[25], or through the use of a specific tetramer of I-A^b and peptide of OVA amino acids 328–337 (I-A^b–OVA(328–337)), which showed their ability to bind cognate peptide presented on self MHC class II (**Supplementary Fig. 3b**,**c**). LI LP OT-II CD4$^+$ T cells in both DTg mice and OT-II mice were CD44$^+$ (**Supplementary Fig. 3c**), consistent with the phenotype of intestinal CD4$^+$ T cells[26,27]. OT-II T cells in DTg mice also had higher expression of the negative regulator CD5, which correlates with TCR autoreactivity[28], than that of MLN or LI LP OT-II T cells in OT-II mice (**Fig. 3b**). Furthermore, CD4$^+$ T cells from OT-II mice stained more brightly after detection with either I-A^b–OVA(328–337) or antibody to $V_\beta5$ (anti-$V_\beta5$) than did those from DTg mice (**Supplementary Fig. 3b**,**c**). This suggested that T cells with high avidity for I-A^b–OVA(328–337) were eliminated in DTg mice, while those with low avidity remained, as reported before[21–23]. Consistent with a published report[22], the thymus, MLNs and LI LP of DTg mice showed enrichment for Foxp3$^+$ T_{reg} cells expressing the $V_\alpha2V_\beta5$ TCR (~28%, 18% and 40%, respectively) relative to their abundance in OT-II mice (**Fig. 3c**,**d**). Indeed, self-reactive $V_\alpha2^{hi}V_\beta5^+$ T cells in the LI LP of DTg mice showed enrichment for Foxp3$^+$ T cells relative to the abundance of Foxp3$^+$ T cells among $V_\alpha2^-V_\beta5^-$ CD4$^+$ T cells (**Fig. 3d**). $V_\alpha2^{hi}V_\beta5^+$ OT-II T cells from DTg mice did not have detectable expression of the transcription factors T-bet, GATA3 or RORγt (**Fig. 3e**).

Splenic CD25$^-$CD4$^+$ T cells from DTg mice underwent less proliferation than did those from OT-II mice when stimulated *in vitro* with BMDCs pulsed with the cognate peptide OVA (329–337), despite the high concentration of peptide we used (**Fig. 3f**), which suggested 'antigen tuning' of the self-reactive TCR[29]. They also failed to secrete IL-17, consistent with their lack of RORγt expression (**Fig. 3e**,**g**). These cells secreted IL-17 only when primed by BMDCs that had phagocytosed B cells that contained TLR ligand and expressed OVA (**Fig. 3g**), consistent with T_H17 differentiation after simultaneous recognition by DCs of TLRs and apoptotic-cell-derived ligands[13,14].

Finally, despite the increased frequency of autoreactive CD4$^+$ T cells, DTg mice did not spontaneously develop autoimmunity and were healthy (data not shown), as noted before[22]. DTg mice did not exhibit altered susceptibility to *C. rodentium* relative to that of wild-type or OT-II mice, according to statistically insignificant differences in bacterial burden and colitis scores after infection (**Supplementary Fig. 4a**,**b**). Additionally, the polyclonal LI LP T_H17 cell response after infection was similar in DTg mice and Act-mOVA mice (**Supplementary**

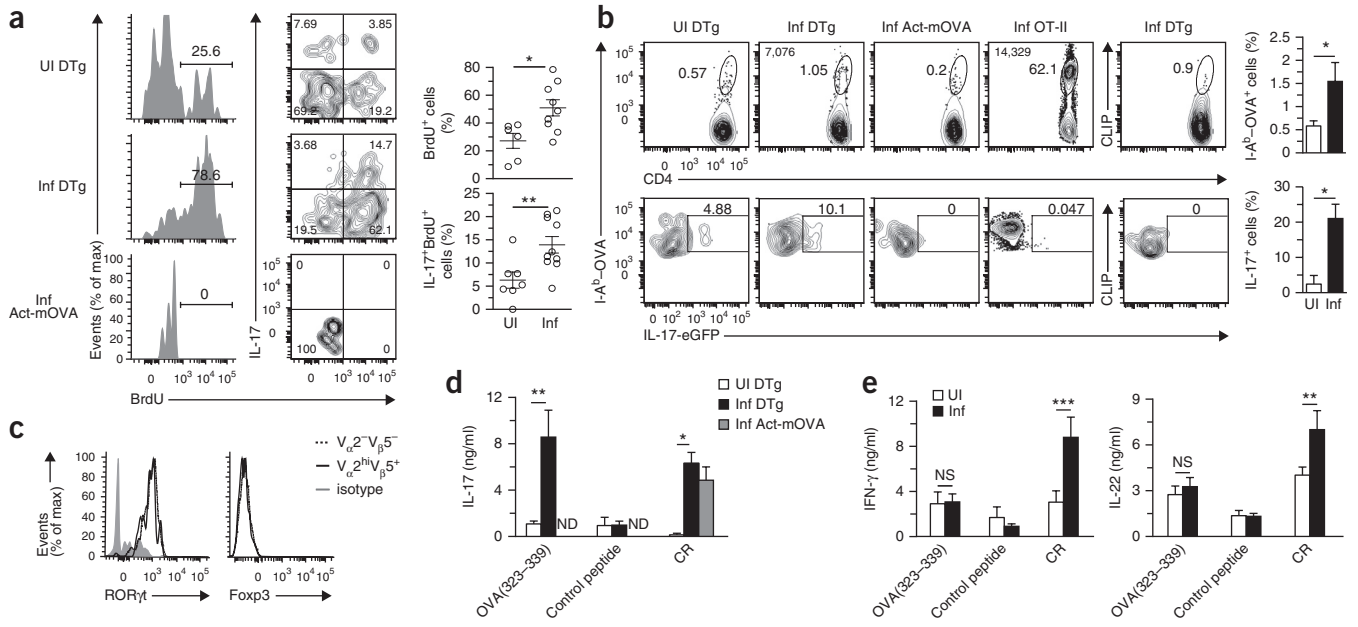

Figure 4 Infection promotes the proliferation of self-reactive CD4$^+$ T cells and their commitment to the T_H17 lineage. (**a**,**b**) Proliferation (left) and IL-17 production (middle) of LI LP $V_\alpha2^{hi}V_\beta5^+$CD4$^+$ T cells (gated on live B220$^-$CD45$^+$CD3$^+$CD4$^+$ cells) in DTg or Act-mOVA mice left uninfected or at day 9 after infection with *C. rodentium* (left margin; numbers above bracketed lines (left), as in **Fig. 2d**). Right, quantification of results at left: each symbol represents an individual mouse; small horizontal lines indicate the mean (± s.d.). (**b**) Flow cytometry (left) of CD4$^+$ T cells (gated as in **a**) from the LI LP of DTg, Act-mOVA or OT-II IL-17A–eGFP mice infected as in **a**, re-stimulated *ex vivo* with PMA plus ionomycin. Numbers adjacent to outlined areas indicate percent I-A^b–OVA tetramer–positive and IL-17A–eGFP$^+$ cells (left four columns) or CLIP (unrelated tetramer)–positive IL-17A–eGFP$^+$ cells (right column); numbers in top left corners indicate mean fluorescence intensity (MFI) of IL-17A–eGFP in the cells outlined. Far right, quantification of results at left. (**c**) Expression of RORγt and Foxp3 by various subsets (key) of IL-17$^+$CD4$^+$ T cells (gated as in **a**) from DTg mice at day 9 after infection with *C. rodentium*, assessed by flow cytometry. (**d**,**e**) ELISA of IL-17 (**d**) or IFN-γ and IL-22 (**e**) in supernatants of CD4$^+$ T cells from the MLNs of mice as in **a** (**d**) or DTg mice treated as in **a** (**e**) (key), re-stimulated *ex vivo* with OVA(323–339), a control peptide or *C. rodentium* (horizontal axis). $^*P \le 0.05$, $^{**}P \le 0.01$ and $^{***}P \le 0.001$ (*t*-test (**a**), Mann-Whitney *U* test (**b**), one-way ANOVA and Dunnet's post-test (**d**,**e**) or Tukey's post-test (**e**, IL-22)). Data are representative of three (**a**,**c**–**e**) or two (**b**) experiments (mean and s.d.) with $n = 7$ mice (UI) or $n = 10$ mice (Inf) (**a**,**e**), $n = 6$ mice (**b**), $n = 9$ mice (**c**), or $n = 6$ mice (UI) or $n = 8$ mice (Inf) (**d**).

Fig. 4c). Thus, DTg mice proved useful for the study of autoreactive CD4$^+$ T cells during an infection that induces host-cell apoptosis.

C. rodentium infection activates self-specific CD4$^+$ T cells

We next investigated whether infection with *C. rodentium* known to induce apoptosis of colonic epithelial cells[13,14] could prime self-reactive CD4$^+$ T cells specific to cellular antigens derived from infected apoptotic cells. We observed a significantly greater frequency of $V_\alpha2^{hi}V_\beta5^+$CD4$^+$ T cells positive for the thymidine analog BrdU in the LI LP of DTg mice after infection (~50%) than in that of uninfected DTg mice (~30%) (**Fig. 4a**). Since *C. rodentium* infection 'preferentially' induces T_H17 cell–mediated immunity[14], we investigated whether self-reactive CD4$^+$ T cells were also able to acquire this phenotype. Notably, ~15% of self-reactive $V_\alpha2^{hi}V_\beta5^+$CD4$^+$ T cells in the LI LP proliferated and produced IL-17 (**Fig. 4a**). We crossed DTg mice to IL-17A–eGFP reporter mice, which have sequence encoding enhanced green fluorescent protein (eGFP) inserted into the *Il17a* locus[17], and tracked endogenous self-reactive CD4$^+$ T cells by tetramer staining (**Fig. 4b**). Consistent with the proliferation and IL-17 production of self-reactive $V_\alpha2^{hi}V_\beta5^+$ CD4$^+$ T cells (**Fig. 4a**), the frequency of I-A^b–OVA(328–337)$^+$ CD4$^+$ T cells from DTg IL-17A reporter mice increased (approximately threefold) after infection with *C. rodentium* relative to their abundance in uninfected DTg IL-17A reporter mice, and this was specific, as we detected no similar increase by staining for an irrelevant tetramer (**Fig. 4b**). Upon infection of Act-mOVA or OT-II mice with *C. rodentium*, I-A^b–OVA(328–337)$^+$CD4$^+$ T cells did not express IL-17, while I-A^b–OVA(328–337)$^+$CD4$^+$ T cells in infected DTg mice included a greater frequency of IL-17–eGFP$^+$ cells than that among their counterparts from uninfected DTg mice (~20% on average; **Fig. 4b**). Self-reactive $V_\alpha2^{hi}V_\beta5^+$ cells had RORγt expression similar to that in non–self-reactive $V_\alpha2^-V_\beta5^-$ IL-17–producing CD4$^+$ T cells, but, notably, they did not express Foxp3 (**Fig. 4c**), which identified these cells as true T_H17 cells. As noted for total LI LP Foxp3$^+$CD4$^+$ T cells (**Supplementary Fig. 2c**), the frequency of self-reactive Foxp3$^+$$V_\alpha2^{hi}V_\beta5^+$ T_{reg} cells and their expression of IL-10 was lower in infected DTg mice and in the progeny of DTg mice crossed to mice with sequence encoding eGFP knocked into the *Il10* locus (**Supplementary Fig. 5a**).

Whereas MLN CD4$^+$ T cells from both infected Act-mOVA mice and infected DTg mice produced IL-17 in response to *C. rodentium* antigens (a *C. rodentium*–specific response), only DTg mice had a population that secreted IL-17 in response to splenocytes pulsed with OVA(323–339) peptide (a self-specific response) but not in response control peptide (**Fig. 4d**), which confirmed the induction of T_H17 cells specific to self antigen in DTg mice. Notably, these cells did not secrete significantly more IFN-γ or IL-22 than did those from uninfected mice or those stimulated with non-cognate peptide (**Fig. 4e**). On the other hand, LI LP *C. rodentium*–specific T_H17 cells secreted IL-22, and a subset of these cells acquired expression of IFN-γ and T-bet (**Fig. 2c** and **Supplementary Fig. 2a**,**b**). This was also observed in *C. rodentium*–specific CD4$^+$ T cells purified from the MLNs of DTg mice (**Fig. 4e**). The types and levels of cytokines produced by *C. rodentium*–specific MLN CD4$^+$ T cells were similar in DTg mice and wild-type mice (**Figs. 2c** and **4d**,**e**), which demonstrated

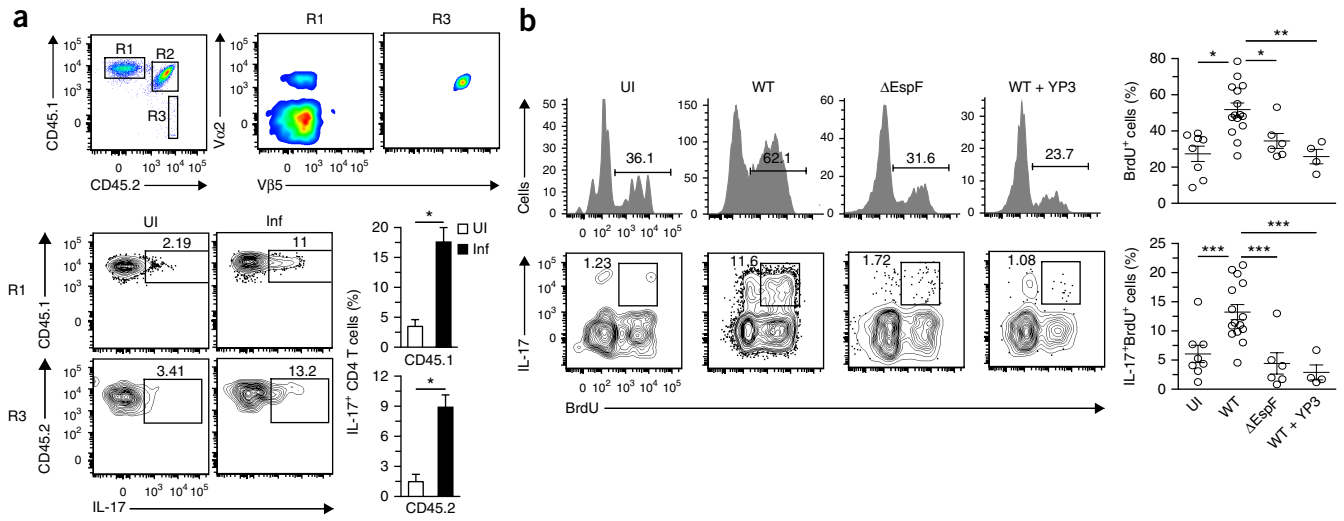

Figure 5 Apoptosis and self-antigen presentation are necessary for the activation of self-reactive T cells. (**a**) Flow cytometry of CD4$^+$ T cells (gated on Aqua$^-$B220$^-$CD3$^+$ cells) from the LI LP of uninfected Act-mOVA (CD45.1$^+$CD45.2$^+$) chimeras reconstituted with bone marrow from OT-II *Tcra*$^{-/-}$ (CD45.2$^+$) mice and wild-type (CD45.1$^+$) mice (top row), and of wild-type (R1) and *Tcra*$^{-/-}$ (R3) OT-II CD4$^+$ T cells (left margin) from chimeras left uninfected or at day 9 after infection with *C. rodentium* (above plots) (bottom left group). Outlined areas (top left) indicate wild-type (R1), endogenous (R2) and *Tcra*$^{-/-}$ (R3) OT-II CD4$^+$ T cell populations; numbers adjacent to outlined areas (bottom left group) indicate percent IL-17$^+$ cells among CD45.1$^+$ or CD45.2$^+$ CD4$^+$ T cells. Bottom right, quantification of results at left. (**b**) Flow cytometry (left) of $V_\alpha2^{hi}V_\beta5^+$ CD4$^+$ T cells (gated on Aqua$^-$B220$^-$CD45$^+$CD3$^+$ cells) from the LI LP of DTg mice left uninfected or at day 9 after infection with wild-type or ΔEspF *C. rodentium* alone or infection with wild-type *C. rodentium* plus treatment with antibody to MHC class II (WT + Y3P) (above plots), followed by re-stimulation *ex vivo* with PMA plus ionomycin. Numbers above bracketed lines (top) indicate percent BrdU$^+$ (proliferated) cells; numbers adjacent to outlined areas (bottom) indicate percent IL-17$^+$BrdU$^+$ cells. Right, quantification of results at left: each symbol represents an individual mouse; small horizontal lines indicate the mean (± s.d.). $^*P \le 0.05$, $^{**}P \le 0.01$ and $^{***}P \le 0.001$ (*t*-test (**b**) or one-way ANOVA with Tukey's post-test (**c**)). Data are representative of three experiments with $n = 7$ mice (**a**) or three independent experiments with $n = 8$ mice (UI) , $n = 15$ mice (WT), $n = 6$ mice (ΔEspF) or two independent experiments with $n = 4$ mice (wild-type + YP3) (**b**).

an intact *C. rodentium*–specific response (**Supplementary Fig. 4**). Collectively, these results demonstrated the generation of a distinct self-reactive T_H17 response alongside a *C. rodentium*–specific T_H17 response after infection.

No antigen mimicry in the activation of self-specific CD4$^+$ T cells

The potential expression of a second TCR due to incomplete allelic exclusion of rearrangements to the *Tcra* locus[25] raised the possibility that self-reactive CD4$^+$ T cells might recognize a microbial antigen. We reconstituted irradiated CD45.1$^+$CD45.2$^+$ Act-mOVA mice with bone marrow from CD45.2$^+$ OT-II *Tcra*$^{-/-}$ mice. Because such mice might be unable to cope with *C. rodentium* infection, chimeras also received bone marrow from CD45.1$^+$ wild-type mice at a ratio of 1:1 (**Supplementary Fig. 5b**). The recipient mice expressed OVA as a self antigen and had CD45.1$^+$ CD4$^+$ T cells with a polyclonal TCR repertoire and CD45.2$^+$ CD4$^+$ T cells that expressed a monoclonal $V_\alpha2V_\beta5$ TCR fixed on a *Tcra*$^{-/-}$ background (**Fig. 5a**). A low frequency of CD45.2$^+$ CD4$^+$ T cells in the LI LP and thymus (**Fig. 5a** and **Supplementary Fig. 5b**) indicated negative thymic selection, as reported in similar models[22]. Notably, infection with *C. rodentium* induced IL-17 production not only by polyclonal CD45.1$^+$ CD4$^+$ T cells but also by the self-reactive CD45.2$^+$ OT-II *Tcra*$^{-/-}$ population (**Fig. 5a**). These data confirmed the conclusion that the $V_\alpha2V_\beta5$ TCR, which is specific to OVA as a self antigen in this model, and not another TCR composed of $V_\beta5$ paired with a different V_α region, was responsible for the activation and differentiation of self-reactive T cells.

Infection-induced apoptosis drives self-reactive T_H17 cells

If the source of self antigen were indeed apoptotic cells, the absence of apoptosis would impair both the proliferation and the T_H17 differentiation of self-reactive CD4$^+$ T cells. Self-reactive CD4$^+$ T cells failed to differentiate into T_H17 cells and, more importantly, were unable to proliferate in mice infected with ΔEspF *C. rodentium* (which cannot induce apoptosis), in contrast to results obtained for mice infected with wild-type *C. rodentium* (**Fig. 5b**). Among $V_\alpha2^{hi}V_\beta5^+$ cells, the frequency of proliferating cells was similar in uninfected mice and mice infected with ΔEspF *C. rodentium* (**Fig. 5b**). Blocking apoptosis during infection with wild-type *C. rodentium* (by treatment with a pan-caspase inhibitor that does not affect T cell activation[13]) also impaired the differentiation of self-reactive CD4$^+$ T cells into T_H17 cells (**Supplementary Fig. 5c**). Blocking presentation by MHC class II during infection with wild-type *C. rodentium* impaired the proliferation and IL-17 production of self-reactive $V_\alpha2^{hi}V_\beta5^+$CD4$^+$ T cells (**Fig. 5b**). These results demonstrated the need for antigen presentation in the activation of self-reactive CD4$^+$ T cells during infection-induced apoptosis.

Infection-associated autoantibody secretion and colitis

The induction of T_H17 cells after colonization with segmented filamentous bacteria or infection with epithelial-cell-adherent bacteria[30] or after model oral vaccination[31] or *C. rodentium* infection[13,30] is accompanied by an increase in intestinal immunoglobulin A (IgA). Autoantibodies are a key characteristic of autoimmune diseases, including those of the gastrointestinal tract[4,32,33]. *C. rodentium* infection induced an increase in serum anti-OVA IgA at day 40 after infection in DTg mice that was not observed in Act-mOVA, wild-type or OT-II mice (**Fig. 6a**). Furthermore, we detected anti-OVA IgG1 in infected DTg mice but not in infected Act-mOVA mice, but the concentrations of anti-OVA IgM were similar in these mice (**Supplementary Fig. 6a**). The appearance of OVA-specific IgA

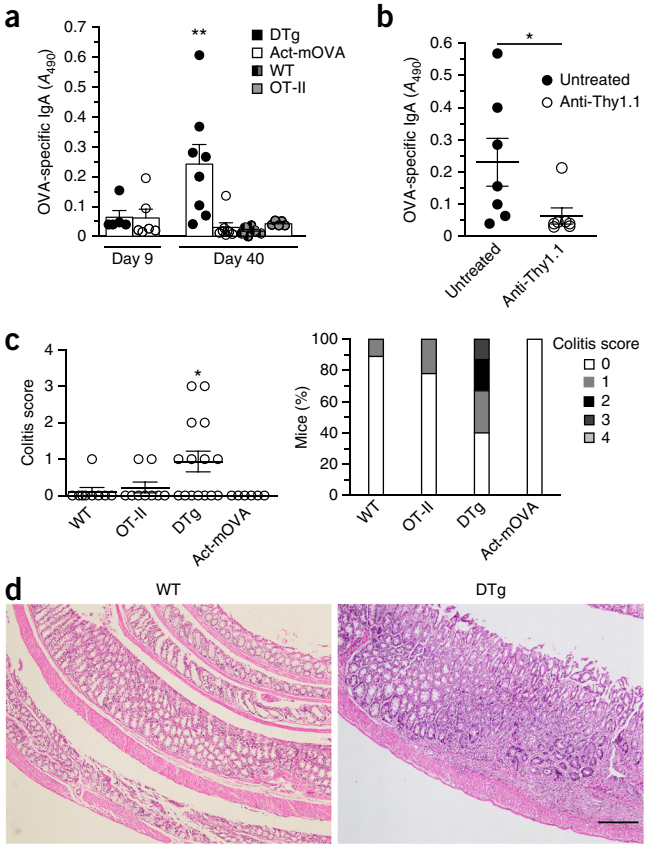

Figure 6 The generation of self-reactive T_H17 cells is associated with a self-reactive IgA response and intestinal pathology. (**a**) Quantification of anti-OVA IgA in the serum of DTg, Act-mOVA, wild-type and OT-II mice (key) on days 9 and 40 after infection with *C. rodentium* (horizontal axis), presented as absorbance at 490 nm (A_{490}). (**b**) Quantification of anti-OVA IgA in Act-mOVA chimeras ($n = 7$) reconstituted with bone marrow from wild-type and OT-II mice and infected with *C. rodentium*, then left untreated or depleted of OT-II T cells with anti-Thy1.1 (horizontal axis; **Supplementary Fig. 6b**), assessed on day 40 after infection (presented as in **a**). (**c**) Colitis scores (left) of wild-type, OT-II, DTg and Act-mOVA mice on day 40 after infection with *C. rodentium* (on a scale of 0 (no change) to 4 (most severe) for inflammation, crypt abscesses, granulomatous inflammation, hyperplasia, mucin depletion, ulceration and crypt loss), and frequency of such mice with each score (right). (**d**) Hematoxylin-and-eosin staining of sections of large intestine from wild-type and DTg mice on day 40 after infection with *C. rodentium*. Scale bar, 250 µm. Each symbol (**a**,**b**,**c**) represents an individual mouse; small horizontal lines (**b**,**c**) indicate the mean (± s.d.). $*P \leq 0.05$ and $**P \leq 0.01$ (one-way ANOVA and Dunnet's post-test (**a**,**c**) or *t*-test (**b**)). Data are representative of three experiments with $n = 6$ mice (DTg and Act-mOVA at day 9; wild-type and OT-II at day 40) or $n = 8$ mice (DTg and Act-mOVA at day 40) (**a**; mean + s.d.), two experiments (**b**) or three experiments with $n = 6$ mice (Act-mOVA), $n = 9$ mice (wild-type and OT-II) or $n = 15$ mice (DTg) (**c**,**d**).

and IgG1 autoantibodies was accompanied by the presence of OVA-specific self-reactive T_H17 cells in DTg mice but not in Act-mOVA mice (**Fig. 4a**,**b**,**d**), suggestive of the provision of help to B cells by T_H17 cells[33].

To address the role of autoreactive $CD4^+$ T cells in autoantibody secretion, we generated Act-mOVA chimeras reconstituted with bone marrow from $Thy1.2^+$ wild-type mice and $Thy1.1^+$ OT-II mice (**Supplementary Fig. 6b**), which allowed specific depletion of OT-II T cells with anti-Thy1.1 before infection with *C. rodentium*. Notably, depleting the mice of OT-II T cells abolished the anti-OVA IgA response (**Fig. 6b**). On the other hand, serum anti-OVA IgM levels were similar in anti-Thy1.1-treated mice and untreated mice, consistent with the T cell–independent nature of the IgM response, while we no longer detected serum anti-OVA IgG1 (**Supplementary Fig. 6c**). Thus, self-reactive T cells were responsible for the generation of class-switched IgA autoantibodies in this model.

Notably, 60% of DTg mice showed colonic neutrophilic and lymphocytic infiltration at day 40 after infection with *C. rodentium*, with foci of aggregation suggestive of a combined acute and chronic inflammatory process, whereas little to no pathology was detected in similarly infected wild-type, OT-II or Act-mOVA mice (**Fig. 6c**,**d**). Various levels of epithelial hyperplasia and depletion of goblet cells were also observed (**Fig. 6c**,**d**). The pathology of the large intestine in the infected DTg mice was not due to an inability to clear bacteria (**Supplementary Fig. 4b**). A milder pathology was observed in chimeric mice after depletion of $Thy1.1^+$ OT-II cells (**Supplementary Fig. 6d**). Therefore, an enteric apoptosis-inducing infection has the potential to elicit intestinal pathology through the generation of a self-reactive T_H17 response (**Supplementary Fig. 6e**).

DISCUSSION

Cumulative evidence has challenged the conclusion that clonal deletion purges the repertoire of self-reactive T cells[34,35]. Comparison of the frequency of self-reactive $CD4^+$ T cells among a normal repertoire in mice lacking or expressing a defined self antigen has shown the persistence of one third of low-affinity self-reactive $Foxp3^+$ or $Foxp3^-$ $CD4^+$ T cells, despite the presence of self antigen[36]. Similar findings have been reported for self-reactive $CD8^+$ T cells[37,38]. Autoreactive T cells have been detected in the peripheral blood of healthy subjects at a frequency similar to that in patients with autoimmune disease[9,34,39]. In the context of autoimmune pathologies (such as celiac disease) with a strong association with polymorphisms in MHC class II molecules, epidemiological and genetic studies have shown that achieving a threshold number of autoreactive T cells is necessary for disease[40,41]. Genetic susceptibility to autoimmunity also includes anomalies in thymic selection and T cell signaling[1,42]. An increasing abundance of self-reactive cells and their progressive acquisition of an effector phenotype directly correlate with disease precipitation[40,41]. Nevertheless, the frequency of self-reactive T cells is small due to thymic deletion or inactivation[35,43], which makes it difficult to study and characterize these cells.

Transgenic expression of a TCR in a context in which its cognate antigen is expressed as self leads to the generation of a low but detectable number of low-affinity self-reactive T cells that overcome thymic tolerance[21–23]. Using this experimental system, we have shown how infection contributed to the differentiation of autoreactive $CD4^+$ T cells into T_H17 cells associated with several autoimmune diseases[44–46]. By eliminating the possibility for self-reactive $CD4^+$ T cells to express TCRs other than the self-reactive TCR, we have shown that the cognate self antigen–TCR interaction was responsible for this activation. In this same model, successful mobilization of a $CD4^+$ T cell response to *C. rodentium* infection demonstrated the preservation of a functional polyclonal T cell repertoire. During an infection that causes host-cell apoptosis, the T_H17 fate of $CD4^+$ T cells is a consequence of innate recognition of infected apoptotic cells, which promotes production of the cytokines TGF-β (in response to apoptosis-induced phosphatidyl serine) and IL-6 (in response to TLR ligands from the infection) by DCs[13,14]. After phagocytosis of infected apoptotic cells, the simultaneous phagosomal compartmentalization of apoptotic cells and microorganisms together with TLR ligands optimally tailors such phagosomes for antigen presentation[11], which provides the opportunity

for both self peptides and non-self peptides to be loaded onto MHC class II molecules.

C. rodentium induces apoptosis as the specific mode for the death of colonic intestinal epithelial cells, and the T_H17 response is considerably impaired in mice infected with ΔEspF *C. rodentium* (which cannot induce apoptosis)[13,14]. Necrosis or pyroptosis are not expected to 'instruct' T_H17 differentiation, mainly because of the inability of these processes to induce the simultaneous secretion of biologically active TGF-β and inflammatory cytokines by DCs[13,14]. Although NLRP3-inflammasome-dependent pyroptosis has been reported in response to *C. rodentium* and, regardless of the expression of some effectors of the pathogenicity island LEE ('locus of enterocyte effacement')[47], the lack of activation of self-reactive $CD4^+$ T cells after infection with ΔEspF *C. rodentium* challenges the proposal of a role for pyroptosis in releasing intact self antigens or driving bystander activation of self-reactive $CD4^+$ T cells. Furthermore, the latter cannot be driven by infection-induced inflammation itself, as indicated by the impaired activation of self-reactive $CD4^+$ T cells after blockade of MHC class II.

Self-reactive T cells are controlled by peripheral $Foxp3^+$ T_{reg} cells[39]. Indeed, autoimmune disease in mice and humans lacking $Foxp3^+CD4^+$ T cells is strong evidence for the presence of self-reactive $CD4^+$ T cells within the normal T cell repertoire[22]. Systemic ablation of T_{reg} cells mediates the activation of $CD4^+$ T cells with specificity to select tissue-restricted self antigens after immunization with the cognate peptide[48]. Intact peripheral tolerance might explain the healthy status of our DTg mice and the absence of an effector phenotype among self-reactive $CD4^+$ T cells at steady state, as well as the moderate intestinal pathology elicited after an infection that induces apoptosis. On the other hand, a decrease in IL-10 and $Foxp3^+CD4^+$ T cells after infection with *C. rodentium* in both DTg mice and wild-type mice, as has been reported before[20], might enable the mobilization of an anti-bacterial T_H17 response and additionally contribute to the activation of self-reactive T cells in our model. One proposed mechanism for the decrease in the abundance of $Foxp3^+CD4^+$ T cells after infection is that secretion of IL-1 during *C. rodentium* infection favors differentiation into T_H17 cells over differentiation into T_{reg} cells during infection[20].

Microbes that adhere to intestinal epithelial cells induce both T_H17 cell differentiation and IgA secretion[30], as has also been shown for *C. rodentium*[13,30]. Notably, we also found a link between differentiation into self-reactive T_H17 cells and IgA production whereby self-reactive IgA produced in response to *C. rodentium* infection was abolished after the deletion of self-reactive $CD4^+$ T cells. Self-reactive T_H17 cells might migrate to germinal centers in the large intestine to interact with B cells and facilitate IgA class switching[49]. Additionally, the enhanced susceptibility of DTg mice to colitis was ameliorated by depletion of self-reactive $CD4^+$ T cells, which would suggest a role for self-reactive T_H17 cells in the development of colitis. Indeed, increased IgA and T_H17 responses have both been associated with inflammatory bowel disease, albeit in the context of the recognition of microbes[30,50]. The colitis observed here was mild, probably because auto-aggression by self-reactive T cells would culminate in full-blown autoimmunity only in the setting of polymorphisms in multiple genes encoding products involved in immunotolerance and immune-system function, consistent with the multifactorial etiology of autoimmune disease[1]. Finally, the link between infection and the activation of autoreactive T cells supports the idea that pathogen tropism could determine the specific localization of autoimmune diseases, despite ubiquitous expression of self antigens[2]. Thus, our study has identified a mechanism by which infection might trigger autoimmune disease in genetically susceptible people and has implications for new therapeutic avenues to limit disease precipitation.

METHODS

Methods and any associated references are available in the online version of the paper.

Note: Any Supplementary Information and Source Data files are available in the online version of the paper.

ACKNOWLEDGMENTS

We thank S. Lira, G. Furtado, H. Xiong, G. Yeretssian, M.K. Jenkins and members of the Blander laboratory for discussions; D. Amsen and R.J. Cummings for critical reading of the manuscript; A. Rialdi for help with statistical analyses; J. Ochando and C. Bare for flow cytometry; A. Soto and M.J. Suarez (the NIH Tetramer Core Facility at Emory University) for I-A^b–OVA(328–337) and control tetramers; H. Xiong (The Icahn School of Medicine at Mount Sinai) for LM-OVA bacteria; A. Morelli (University of Pittsburgh) for 1H3.1 mice; B. Finlay and M. Croxen (University of British Columbia) for wild-type and ΔEspF *C. rodentium* and plasmid pMAC5; H.P. Schweizer (Colorado State University) for plasmid pTNS2; D. Mazel (Institut Pasteur) for MFDpir bacteria; and I. Marazzi, V. Verhasselt, S.E.F. Campisi, G.C. Chiesa, Jr., M.A. Blander, S.J. Blander and the late L. Mayer for advice and support. Supported by the National Institute of Diabetes and Digestive and Kidney Diseases (DK072201 to J.M.B.), the National Institute of Allergy and Infectious Diseases (AI073899, AI080959 and AI095245 to J.M.B.), the Arthritis Foundation (L.C.), the Crohn's and Colitis Foundation of America (G.B.), the Burroughs Wellcome Fund (J.M.B.), the Irma Hirschl and Monique Weill-Caulier Charitable Trust Funds (J.M.B.), the American Cancer Society (J.M.B.) and the Leukemia and Lymphoma Society (J.M.B.).

AUTHOR CONTRIBUTIONS

L.C. and J.M.B designed and directed the study and wrote the manuscript; L.C. conducted all experiments; G.B. assisted with T cell–sorting experiments; Y.D. conducted the histological and pathological assessments of colonic tissues; E.E. and R.A.F. provided the IL-17–eGFP reporter mice; and J.M.B conceived of the study.

COMPETING FINANCIAL INTERESTS

The authors declare no competing financial interests.

1. Cho, J.H. & Gregersen, P.K. Genomics and the multifactorial nature of human autoimmune disease. *N. Engl. J. Med.* **365**, 1612–1623 (2011).
2. Marrack, P., Kappler, J. & Kotzin, B.L. Autoimmune disease: why and where it occurs. *Nat. Med.* **7**, 899–905 (2001).
3. Sakaguchi, S., Powrie, F. & Ransohoff, R.M. Re-establishing immunological self-tolerance in autoimmune disease. *Nat. Med.* **18**, 54–58 (2012).
4. Suurmond, J. & Diamond, B. Autoantibodies in systemic autoimmune diseases: specificity and pathogenicity. *J. Clin. Invest.* **125**, 2194–2202 (2015).
5. Cho, J.H. & Feldman, M. Heterogeneity of autoimmune diseases: pathophysiologic insights from genetics and implications for new therapies. *Nat. Med.* **21**, 730–738 (2015).
6. Blander, J.M., Torchinsky, M.B. & Campisi, L. Revisiting the old link between infection and autoimmune disease with commensals and T helper 17 cells. *Immunol. Res.* **54**, 50–68 (2012).
7. Pordeus, V., Szyper-Kravitz, M., Levy, R.A., Vaz, N.M. & Shoenfeld, Y. Infections and autoimmunity: a panorama. *Clin. Rev. Allergy Immunol.* **34**, 283–299 (2008).
8. Sfriso, P. *et al.* Infections and autoimmunity: the multifaceted relationship. *J. Leukoc. Biol.* **87**, 385–395 (2010).
9. Rosenblum, M.D., Remedios, K.A. & Abbas, A.K. Mechanisms of human autoimmunity. *J. Clin. Invest.* **125**, 2228–2233 (2015).
10. Root-Bernstein, R. & Fairweather, D. Complexities in the relationship between infection and autoimmunity. *Curr. Allergy Asthma Rep.* **14**, 407 (2014).
11. Blander, J.M. & Medzhitov, R. Toll-dependent selection of microbial antigens for presentation by dendritic cells. *Nature* **440**, 808–812 (2006).
12. Nair-Gupta, P. *et al.* TLR signals induce phagosomal MHC-I delivery from the endosomal recycling compartment to allow cross-presentation. *Cell* **158**, 506–521 (2014).
13. Torchinsky, M.B., Garaude, J., Martin, A.P. & Blander, J.M. Innate immune recognition of infected apoptotic cells directs T_H17 cell differentiation. *Nature* **458**, 78–82 (2009).
14. Brereton, C.F. & Blander, J.M. The unexpected link between infection-induced apoptosis and a TH17 immune response. *J. Leukoc. Biol.* **89**, 565–576 (2011).
15. Hirota, K. *et al.* Fate mapping of IL-17-producing T cells in inflammatory responses. *Nat. Immunol.* **12**, 255–263 (2011).

16. Mowat, A.M. & Agace, W.W. Regional specialization within the intestinal immune system. *Nat. Rev. Immunol.* **14**, 667–685 (2014).
17. Esplugues, E. *et al.* Control of T_H17 cells occurs in the small intestine. *Nature* **475**, 514–518 (2011).
18. McGeachy, M.J. *et al.* TGF-β and IL-6 drive the production of IL-17 and IL-10 by T cells and restrain T_H-17 cell–mediated pathology. *Nat. Immunol.* **8**, 1390–1397 (2007).
19. Berer, K. *et al.* Commensal microbiota and myelin autoantigen cooperate to trigger autoimmune demyelination. *Nature* **479**, 538–541 (2011).
20. Basu, R. *et al.* IL-1 signaling modulates activation of STAT transcription factors to antagonize retinoic acid signaling and control the T_H17 cell–iT_{reg} cell balance. *Nat. Immunol.* **16**, 286–295 (2015).
21. Marks, B.R. *et al.* Thymic self-reactivity selects natural interleukin 17–producing T cells that can regulate peripheral inflammation. *Nat. Immunol.* **10**, 1125–1132 (2009).
22. Simons, D.M. *et al.* How specificity for self-peptides shapes the development and function of regulatory T cells. *J. Leukoc. Biol.* **88**, 1099–1107 (2010).
23. Zehn, D. & Bevan, M.J. T cells with low avidity for a tissue-restricted antigen routinely evade central and peripheral tolerance and cause autoimmunity. *Immunity* **25**, 261–270 (2006).
24. Malissen, M. *et al.* Regulation of TCR α and β gene allelic exclusion during T-cell development. *Immunol. Today* **13**, 315–322 (1992).
25. Padovan, E. *et al.* Expression of two T cell receptor α chains: dual receptor T cells. *Science* **262**, 422–424 (1993).
26. Jalkanen, S., Nash, G.S., De los Toyos, J., MacDermott, R.P. & Butcher, E.C. Human lamina propria lymphocytes bear homing receptors and bind selectively to mucosal lymphoid high endothelium. *Eur. J. Immunol.* **19**, 63–68 (1989).
27. Shimizu, Y., Van Seventer, G.A., Siraganian, R., Wahl, L. & Shaw, S. Dual role of the CD44 molecule in T cell adhesion and activation. *J. Immunol.* **143**, 2457–2463 (1989).
28. Mandl, J.N., Monteiro, J.P., Vrisekoop, N. & Germain, R.N. T cell-positive selection uses self-ligand binding strength to optimize repertoire recognition of foreign antigens. *Immunity* **38**, 263–274 (2013).
29. Grossman, Z. & Paul, W.E. Autoreactivity, dynamic tuning and selectivity. *Curr. Opin. Immunol.* **13**, 687–698 (2001).
30. Atarashi, K. *et al.* Th17 cell induction by adhesion of microbes to intestinal epithelial cells. *Cell* **163**, 367–380 (2015).
31. Fonseca, D.M. *et al.* Microbiota-dependent sequelae of acute infection compromise tissue-specific immunity. *Cell* **163**, 354–366 (2015).
32. Di Sabatino, A., Lenti, M.V., Giuffrida, P., Vanoli, A. & Corazza, G.R. New insights into immune mechanisms underlying autoimmune diseases of the gastrointestinal tract. *Autoimmun. Rev.* **14**, 1161–1169 (2015).
33. Sweet, R.A., Lee, S.K. & Vinuesa, C.G. Developing connections amongst key cytokines and dysregulated germinal centers in autoimmunity. *Curr. Opin. Immunol.* **24**, 658–664 (2012).
34. Richards, D.M., Kyewski, B. & Feuerer, M. Re-examining the nature and function of self-reactive t cells. *Trends Immunol.* **37**, 114–125 (2016).
35. Hogquist, K.A. & Jameson, S.C. The self-obsession of T cells: how TCR signaling thresholds affect fate 'decisions' and effector function. *Nat. Immunol.* **15**, 815–823 (2014).
36. Moon, J.J. *et al.* Quantitative impact of thymic selection on $Foxp3^+$ and $Foxp3^-$ subsets of self-peptide/MHC class II-specific $CD4^+$ T cells. *Proc. Natl. Acad. Sci. USA* **108**, 14602–14607 (2011).
37. Yu, W. *et al.* Clonal deletion prunes but does not eliminate self-specific αβ $CD8^+$ T lymphocytes. *Immunity* **42**, 929–941 (2015).
38. Rizzuto, G.A. *et al.* Self-antigen-specific $CD8^+$ T cell precursor frequency determines the quality of the antitumor immune response. *J. Exp. Med.* **206**, 849–866 (2009).
39. Walker, L.S. & Abbas, A.K. The enemy within: keeping self-reactive T cells at bay in the periphery. *Nat. Rev. Immunol.* **2**, 11–19 (2002).
40. Abadie, V., Sollid, L.M., Barreiro, L.B. & Jabri, B. Integration of genetic and immunological insights into a model of celiac disease pathogenesis. *Annu. Rev. Immunol.* **29**, 493–525 (2011).
41. Vader, W. *et al.* The HLA-DQ2 gene dose effect in celiac disease is directly related to the magnitude and breadth of gluten-specific T cell responses. *Proc. Natl. Acad. Sci. USA* **100**, 12390–12395 (2003).
42. Ito, Y. *et al.* Detection of T cell responses to a ubiquitous cellular protein in autoimmune disease. *Science* **346**, 363–368 (2014).
43. Klein, L., Kyewski, B., Allen, P.M. & Hogquist, K.A. Positive and negative selection of the T cell repertoire: what thymocytes see (and don't see). *Nat. Rev. Immunol.* **14**, 377–391 (2014).
44. Burkett, P.R., Meyer zu Horste, G. & Kuchroo, V.K. Pouring fuel on the fire: Th17 cells, the environment, and autoimmunity. *J. Clin. Invest.* **125**, 2211–2219 (2015).
45. Ghoreschi, K., Laurence, A., Yang, X.P., Hirahara, K. & O'Shea, J.J. T helper 17 cell heterogeneity and pathogenicity in autoimmune disease. *Trends Immunol.* **32**, 395–401 (2011).
46. Kleinewietfeld, M. & Hafler, D.A. The plasticity of human Treg and Th17 cells and its role in autoimmunity. *Semin. Immunol.* **25**, 305–312 (2013).
47. Gurung, P. *et al.* FADD and caspase-8 mediate priming and activation of the canonical and noncanonical Nlrp3 inflammasomes. *J. Immunol.* **192**, 1835–1846 (2014).
48. Legoux, F.P. *et al.* $CD4^+$ T cell tolerance to tissue-restricted self antigens is mediated by antigen-specific regulatory T cells rather than deletion. *Immunity* **43**, 896–908 (2015).
49. Hirota, K. *et al.* Plasticity of T_H17 cells in Peyer's patches is responsible for the induction of T cell-dependent IgA responses. *Nat. Immunol.* **14**, 372–379 (2013).
50. Kazemi-Shirazi, L. *et al.* IgA autoreactivity: a feature common to inflammatory bowel and connective tissue diseases. *Clin. Exp. Immunol.* **128**, 102–109 (2002).

ONLINE METHODS

Mice and mouse-related methods. C57Bl/6J, C57BL/6.Ly5.1 (CD45.1), Act-mOVA (C57BL/6-Tg(CAG-OVA)916Jen/J), OT-II (B6.Cg-Tg(TcraTcrb)425Cbn/J), IL-10–eGFP (B6.129S6-*Il10tm1Flv*/J), CD11c-DTR/GFP and *Tcra*$^{-/-}$ mice were purchased from The Jackson Laboratories. These strains and combinations thereof were bred in the mouse facility of the Icahn School of Medicine at Mount Sinai. IL-17A–eGFP × FoxP3-mRFP mice were previously described[17]. 1H3.1 mice were previously described[51].

Chimeric mice were generated after two rounds of lethal irradiation with 600 rads. 24 h later, irradiated mice were reconstituted by intravenous injection of T cell–depleted bone marrow (1×10^6 to 4×10^6 cells) isolated from various strains of mice. T cells were depleted by incubation with an anti-CD3ε (clone 145-2C11, BioLegend) phycoerythrin (PE)-conjugated antibody, followed by anti-PE magnetic microbeads positive selection (Miltenyi biotec), according to the manufacturer's instructions. Cells in the flow-through were counted and injected into irradiated mice. For mixed bone marrow chimeric mice, we used a ratio of 1:1 of cells. Chimeric mice were studied 8 weeks after bone marrow transplantation.

For the anti-I-A^b treatments, monoclonal antibody YP3 was purchased from Bio X Cell. Mice were injected intraperitoneally with 0.5 mg of antibody 2 h before and after infection, and with 1 mg at 24, 48 and 72 h after infection. Anti-Thy1.1 monoclonal antibody (clone 19E12, Bio X Cell) was injected intraperitoneally at the dose of 0.5 mg 24 h before infection. 0.4 mg of Q-VD-OPH (SM Biochemicals) were injected intraperitoneally at 90 min, 24 h and 48 h after infection.

To deplete CD11c$^+$ cells, CD11c-DTR or chimeric mice reconstituted with CD11c-DTR bone marrow cells were injected intraperitoneally with 4 ng/g of weight with diphtheria toxin (DT, Calbiochem) in PBS 24 h before infection and daily after infection.

All mice were kept under specific pathogen-free conditions in the animal care facility at the Icahn School of Medicine at Mount Sinai. Both male and female mice were studied at 6–12 weeks of age. For experiments involving comparisons among OT-II, Act-mOVA and DTg mice, only littermates were used. For experiments involving comparisons among chimeras, mice with different genotypes and/or bone marrow donors were co-housed after irradiation and throughout the study. In all experiments, mice were randomly assigned to the different groups (uninfected, infected, treated and untreated). All groups of mice included both males and females in comparable numbers and were processed identically throughout the whole experiment (housed on the same shelf in the same room, and all procedures performed at the same time). Investigators were not blinded to sample identity for this study, except for the histological analysis (Microscopic Examination of Colons, below).

Animal numbers were empirically determined as the minimum needed to obtain statistical significance and validate reproducibility, accordingly with our IACUC approved protocol. All experiments were approved by the institutional animal care and use committee and carried out in accordance with the 'Guide for the Care and Use of Laboratory Animals' (NIH publication 86-23, revised 1985).

Bacteria and infection of mice. After 6 h of starvation, mice were orogastrically infected with 1×10^9 or 1×10^{10} wild-type or ΔEspF *C. rodentium* (strain DBS100), respectively. ΔEspF *C. rodentium* is known to induce apoptosis of infected target cells[13,52–54]. We rendered these strains resistant to chloramphenicol by bacterial conjugation using the plasmid pMAC5 containing the mini Tn7 transposon that inserted the antibiotic resistance downstream of the *glmS* gene[55], as previously described[56,57]. pMAC5 was electroporated into MFDpir bacteria followed by a tri-parental mating with MFDpir expressing pMAC5 + MFDpir expressing pTNS2 + *C. rodentium* DBS100, where the pTNS2 plasmid had the *tnsABCD* encoding for the Tn*7* transposase. Neither pMAC5 nor pTNS2 plasmids can replicate in *C. rodentium*. Conjugation was performed overnight in lysogeny broth (LB) medium supplemented with diaminopimelic acid (DAP, Sigma), necessary for the growth of the MFDpir strain. Chloramphenicol resistant DBS100 where transposition occurred were then counter-selected in presence of the antibiotic and in absence of DAP to eliminate MFDpir bacteria. For experiments, bacteria were grown to exponential phase in LB medium supplemented with chloramphenicol (20 μg/ml), then washed and resuspended in 200 μl of phosphate-buffered saline (PBS) before gavage. To determine *C. rodentium* burdens in the stool or colon, stools and colons were weighed, homogenized in water, plated in MacConkey agar plates supplemented with chloramphenicol (20 μg/ml), and pink colonies were counted after incubation for 24 h at 37 °C. Bacterial colony forming units (CFU) were normalized to stool and colon weight.

Recombinant *E. coli* expressing a Curlin-Eα fusion protein, previously described[11,12], was prepared by growing *E. coli* to an optical density at 600 nm (OD_{600}) of 0.6 and adding 0.2 mM IPTG (for induction of fusion proteins) for an additional 6 h of culture. Bacteria were then diluted in PBS to an OD_{600} of 0.6, killed by heating at 60 °C for 1 h. 1×10^9 heat-killed bacteria were then resuspended in PBS and injected intravenously into mice that had previously been anesthetized by isoflurane inhalation.

Cell isolation. Lamina propria lymphocytes (LPLs) were isolated from the large intestine as previously described[13] with some modifications. Fragments of intestines were flushed with PBS, cut longitudinally, placed in 50-ml conical tubes, and washed several times in PBS by vortexing at maximum setting for 15–20 s. Tissues were then removed and placed in 50-ml conical tubes containing 25 ml of RPMI (Sigma), 5% FBS (FBS) (Sigma), 1 mM DTT and 3 mM EDTA, then placed on a rocker at 37 °C for 35 min followed by vortexing extensively at maximum setting. After PBS washing, cells were successively transferred in 7 ml of RPMI, 5% FBS, 1.6 mg/ml collagenase D (Roche), 20 μg/ml DNase (Roche), cut into small pieces and incubated for 1 h on a rocker at 37 °C before homogenization using a 20g syringe. Tissue suspensions were then filtered through a 70 μm cells strainer (BD Falcon), pelleted, resuspended in a 40% isotonic Percoll solution (GE Healthcare), and underlaid with an 80% isotonic Percoll solution. After 20 min of centrifugation at 2,800 r.p.m., mononuclear cells were recovered at the 40–80% interface and washed.

Single-cell suspensions were prepared from the thymus, spleen and MLNs by pressing the tissues through a 70 μm cell strainer followed by homogenization using a 20g syringe and from the bone marrow by flushing the long bones with PBS.

***Ex-vivo* re-stimulation after primary stimulation *in vivo* with *C. rodentium* infection.** For non–antigen-specific re-stimulation, cells were resuspended in complete IMDM (Sigma) (i.e., supplemented with 10% FBS, 100 μg/ml penicillin, 100 μg/ml streptomycin, 2 mM L-glutamine, 10 mM HEPES, and 1 nM sodium pyruvate) with 0.1 μg/ml phorbol 12-myristate 13-acetate (PMA, Sigma), 0.5 μg/ml ionomycin calcium salt, from *Streptomyces conglobatus* (Sigma), and 10 μg/ml brefeldin A, from *Eupenicillium brefeldanium* (Sigma), and incubated for 4–6 h at 37 °C.

For antigen-specific re-stimulation, splenocytes from C57BL/6J CD45.1$^+$ mice were used as antigen-presenting cells (APCs) after CD3$^+$ T cell depletion by incubation with anti-CD3 PE-conjugated antibody (clone 145-2C11; BioLegend), followed by anti-PE magnetic microbeads positive selection (Miltenyi biotec), according to the manufacturer's protocol. Cells from the flow-through were counted, resuspended at 1×10^7 cells/ml in complete IMDM and incubated with 200 μg of *C. rodentium* or *L. monocytogenes* lysates, or 10 μg/ml of the peptides. APCs were plated in 96-well round-bottom plates at 5×10^5 cells/well for LPL or 1×10^6 cells/well for MLN cells, and incubated for 1–2 h at 37 °C.

For intracellular staining, LPL and MLN cells were added to culture in the presence of 10 μg/ml brefeldin A for an additional 6 h. For cytokine quantification by ELISA, CD4$^+$ T cells from MLN were purified by negative selection using Dynal Mouse CD4 Negative selection kit (Invitrogen Dynal) and plated at 2×10^6 cells/well with antigen-pulsed APCs. Supernatants were collected for analysis at 48 h.

For isolation of CD4$^+$ T cells for adoptive transfer or *in vitro* antigen-presentation assays, splenocytes from OT-II or 1H3.1 mice were incubated with anti-CD4 magnetic microbeads for CD4$^+$ T cell positive selection (Miltenyi biotec), according to the manufacturer's instructions. A mixture of 5×10^5 OT-II CD4$^+$ T cells and 5×10^5 1H3.1 CD4$^+$ T cells was adoptively transferred into the chimeric mice.

Antigens. To prepare bacterial lysates, wild-type *C. rodentium* (strain DBS100) and ΔLLO *ΔflaA L. monocytogenes* (strain 10403s, double deficient in listeriolysin O and flagellin) were cultured in LB and brain-heart–infusion

(BHI) broth, respectively, until exponential phase, then washed several times in PBS to eliminate medium. After resuspension in 1 ml PBS + protease inhibitors (Roche), bacteria were sonicated on ice, then centrifuged 30 min at 13,000 r.p.m. Supernatants were collected and filtered using membrane filters with 0.2 µm pore size (Millipore). Protein concentrations were determined using the Bradford Protein Assay (Bio-Rad). OT-II peptide, OVA(323–339) (sequence ISQAVHAAHAEINEAGR) and OVA(329–337) (sequence AAHAEINEA) were purchased from the Proteomics Resource Center of The Rockefeller University. GFP(26–39) (sequence HDFFKSAMPEGYVQE; control peptide) and Eα(52–68)(sequence ASFEAQGALANIAVDKA) peptides were purchased from Abgent.

Antibodies, tetramers, BrdU and CFSE labeling. For flow cytometry, antibodies to the following were purchased from eBioscience and were all used at a dilution of 1:100: anti-mouse CD45.1 (clone A20, cat# 17-0453-81 or 12-0453-82), CD44 (clone IM7, cat# 48-0441-82 or 56-0441-82), $V_{\alpha}2$ (clone B20.1, cat# 48-5812-80 or 12-5812-82), CD5 (clone 53-7.3, cat# 17-0051-81 or 48-0051-82), CD25 (clone PC61.5, cat# 17-0251-81 or 53-0251-82), CD8β (clone eBioH35-17.2, cat# 17-0083-81), CD16/32 (clone 93, cat# 14-0161-82), Thy 1.1 (clone HIS51, cat# 48-0900-82), TCRβ (clone H57-597, cat# 11-5961-82), IL-17A (clone eBio17B7, cat# 25-7177-82), IFN-γ (clone XMG1.2, cat# 12-7311-82 or 17-7311-82), Foxp3 (clone FJK-16s, cat# 48-5773-80 or 50-5773-80), RORγt (clone B2D, cat# 12-6981-82 or 17-6981-82) and T-bet (clone 4B10, cat# 50-5825-80 or 45-5825-82). We purchased antibodies to the following from BioLegend: mouse CD4 (clone RM4-5, cat# 100528 or 100510), CD45 (clone 30-F11, cat# 103116), CD3ε (clone 145-2C11, cat# 100330 or 100312), B220 (clone RA3-6B2, cat# 103226 or 103247) and IL-22 (clone Poly5164, cat# 516406). Anti-mouse V_{β}5.1/5.2 TCR (clone MR9-4, cat# 553189) and anti-mouse CD45.2 (clone 104, cat# 580693) were obtained from BD Bioscience. Rabbit polyclonal antibody to GFP (eBioscience, clone 5F12.4, cat# 13-6498-82) was used for intracellular staining in cells purified from IL-10–eGFP and IL-17A–eGFP × FoxP3-mRFP. Dead cells were discriminated in all experiments using LIVE/DEAD Fixable Aqua Dead Cell stain kit (Molecular Probes by Life technologies, used at 1:1000). PE- or allophycocyanin-conjugated I-A^b–HAAHAEINEA tetramer was used to stain OT-II $CD4^+$ T cells[28] and I-A^b–PVSKMRMATPLLMQA tetramer was used as a negative control. Both tetramers were provided by the NIH Tetramer Core Facility and used at a concentration of 20 µg/ml.

For surface staining, cells were suspended in PBS, 2% FBS, anti-mouse CD16/32 (clone 93, cat# 14-0161-82), 2% mouse serum (Jackson laboratories), 2% rat serum (Jackson laboratories) and 0.1% NaN_3. For intracellular staining, cells were fixed in Fixation/Permeabilization buffer (eBioscience) and stained in Perm/Wash buffer (eBioscience).

For the *in vivo* proliferation experiments, mice were injected daily intraperitoneally with 1 mg of BrdU (5-bromo-2′-deoxyuridine; Sigma) starting from day 1 after infection. BrdU Flow kit (BD Pharmingen) was used to detect intracellular BrdU incorporation according to the manufacturer's instructions. For carboxyfluorescein diacetate succinimidyl ester (CFSE) labeling, cells were resuspended at 2×10^6 cells/well in PBS with 5 µM CFSE (eBioscience) for 10 min at 37 °C and then washed.

Acquisition of stained cells was made with a BD LSRFortessa flow cytometer (BD Bioscience) and data were analyzed with FlowJo software (Treestar).

ELISA. Supernatants from cell cultures were collected at the times indicated for each experiment in the figure legends. The following ELISA monoclonal antibody (mAb) pairs were used: anti-mouse IL-17 (clones TC11-18H10/TC11-8H4.1, BD Biosciences) and IFN-γ (AN-18/R4-6A2, BD Biosciences). All antibodies were used at 1.5 µg/ml for capture and detection. The recombinant cytokines used as standards were purchased from Peprotech. Detection antibodies were all biotinylated. Streptavidin-conjugated horseradish peroxidase (HRP) was added and visualized by *o*-phenylenediamine dihydrochloride (SIGMA) (from tablets) or 3,3′, 5,5′-tetramethylbenzidine solution (TMB, KPL). IL-22 was measured using the Quantikine ELISA mouse/rat IL-22 kit. Supernatants were incubated undiluted or diluted in polystyrene microtiter plates (Nunc), except for IL-22 ELISA, for with the plate was included in the kit. Absorbance at 490 nm or 450 nm was measured with a 'tunable' microplate reader (VersaMax, Molecular Devices). Cytokine supernatant concentrations were calculated by extrapolating absorbance values from standard curves, for which known concentrations were plotted against absorbance using SoftMax Pro 5 software.

Serum immunoglobulin titers. Mice were anesthetized by isoflurane inhalation and then bled retroorbitally using heparinized micro-hematocrit capillary tubes (Fisherbrand). 20–50 µl of blood were collected in 1 ml Eppendorf tubes and centrifuged for 10 min at 10,000 r.p.m. to separate the serum. Serum immunoglobulin titers were measured by ELISA. Polystyrene microtiter plates (Nunc) were coated overnight with 50 µg/ml of ovalbumin (OVA) protein (Sigma), then washed and blocked with bovine serum albumin (1%). Serum samples were applied at 1:5 dilution, and incubated for 3 h at room temperature, then washed and incubated with alkaline-phosphatase-goat-anti-mouse IgM, IgA, IgG1(all from SouthernBiotech SBA Clonotyping System-HRP kit, cat# 5300-05B, dilution 1:100) developed by the addition of *p*-nitrophenyl phosphate solution (Sigma-Aldrich). Optical density (OD) at 490 nm was measured using a tunable microplate reader (VersaMax, Molecular Devices).

***In vitro* antigen-presentation assay.** Bone marrow (BM)-derived GM-CSF DC cultures were grown in 24 well plates as previously described[11,13] in RPMI supplemented with GM-CSF and 5% FBS, plus 100 µg/ml penicillin, 100 µg/ml streptomycin, 2 mM L-glutamine, 10 mM HEPES, 1 nM sodium pyruvate, 1× MEM nonessential amino acids, and 2.5 µM β-mercaptoethanol (all SIGMA). Different phagocytic cargo as indicated below or peptides were added to the culture on day 5. OVA(329–337) and Eα(52–68) peptides were added at 1 µg/ml.

Phagocytic cargo. For experiments with bacteria, recombinant OVA-expressing *Listeria monocytogenes* (LM-OVA) were cultured in BHI medium until exponential phase, then washed several times in PBS to eliminate medium. Before addition to BMDCs, LM-OVA were killed by incubation for 2 h at 37 °C in PBS containing 50 µL of ampicillin. Recombinant *E. coli* expressing a flagellin-ovalbumin or Curlin-Eα fusion protein (*E. coli*-OVA and *E.coli*-Eα, respectively), previously described[11,12], were prepared by growing *E. coli* to an optical density at 600 nm (OD_{600}) of 0.6 and adding 0.2 mM IPTG (for induction of fusion proteins) for an additional 6 h of culture. Bacteria were then diluted in PBS to an OD_{600} of 0.6, and then killed by heating at 60 °C for 1 h. All bacterial cargo were added to BMDC at a ratio of 1:100 (DC/bacteria) for 6 h before T cells were added. For experiments with apoptotic cells, the A20 B cell line was obtained from the ATCC and splenic B cells from Act-mOVA BALB/c mice were purified using the anti-CD19 magnetic microbeads for B cell positive selection (Miltenyi biotec), according to the manufacturer's instructions. The A20 B cell line was confirmed to be mycoplasma free. A20 and B cells were cultured in RPMI medium (Sigma), supplemented with 10% FBS, 100 µg/ml penicillin, 100 µg/ml streptomycin, 2 mM L-glutamine, 10 mM HEPES, and 1 nM sodium pyruvate. Cells used in this study were not contaminated by mycoplasma. Apoptosis was induced by culturing with 0.5 µL anti-CD95 (clone Jo2; BD Biosciences) for 2 h (A20 cells) or by UV irradiation at 350 mJ (B cells). For experiments with infected apoptotic cells, LM-OVA bacteria were cultured until exponential phase, then washed and incubated with A20 cells at MOI = 100 for 8 h. 50 µg/ml of ampicillin (to kill all the extracellular bacteria) and anti-CD95 were then added to the culture for an additional 2 h. LPS-B cell blasts were generated by adding to the cell culture 25 µg/ml LPS (from *Escherichia coli*, serotype 055:B5, L-2880, SIGMA). Infected A20 cells and LPS blasts were washed three times in PBS, and then added to BMDC cultures. Both uninfected and infected apoptotic cargo were added to BMDC at a ratio of 1:2 (DC/apoptotic cells) for 8 h before adding $CD4^+$ T cells.

$CD4^+$T cells. $CD4^+$ T cells were purified as described above, incubated for 10 min at 37 °C with 2.5 µM CFSE in PBS, washed, then suspended in IMDM complete medium and co-cultured with BMDC for 5 d.

Microscopy of colons. For histological analyses, the colons were removed, cut open along the lengths and fixed in 10% formalin overnight. Embedding in paraffin blocks and staining with H&E were conducted by the Biorepository and Pathology Dean's CoRE at the the Icahn School of Medicine at Mount Sinai and untreated mice were used as controls. Microscopic sections were analyzed in a blinded fashion by the same pathologist (Y.D.). A number was randomly assigned by the investigator to discriminate each section, which was then submitted for analysis as 'section 1', 'section 2' etc. No information about treatments and mouse genotypes was communicated to the pathologist.

doi:10.1038/ni.3512

Colons were graded semiquantitatively as 0 (no change) to 4 (most severe) for the following inflammatory lesions: severity of chronic inflammation, crypt abscesses, and granulomatous inflammation; and for the following epithelial lesions: hyperplasia, mucin depletion, ulceration, and crypt loss. Results are presented as the mean of the grades ± s.d. of affected mice. In addition, the depth of the inflammatory process into the large intestinal wall was categorized as extending into the mucosa, the submucosa, or the tunica muscularis or as being transmural (extending to the serosa)[58,59].

Statistical analysis. Statistical analyses were performed using GraphPad Prism. We first calculated the Gaussian distribution of the data using the Kolmogorov-Smirnov test. When two groups were compared, a *t*-test (Gaussian distribution) or Mann-Whitney test (no Gaussian distribution) was used. When several groups were compared, we used a one-way ANOVA test followed by Tukey's (Gaussian distribution) or Dunnet's (no Gaussian distribution) *post-hoc* test. $P \leq 0.05$ was considered significant.

51. Viret, C. & Janeway, C.A. Jr. Functional and phenotypic evidence for presentation of Eα 52-68 structurally related self-peptide(s) in I-Eα-deficient mice. *J. Immunol.* **164**, 4627–4634 (2000).
52. Nagai, T., Abe, A. & Sasakawa, C. Targeting of enteropathogenic *Escherichia coli* EspF to host mitochondria is essential for bacterial pathogenesis: critical role of the 16th leucine residue in EspF. *J. Biol. Chem.* **280**, 2998–3011 (2005).
53. Nougayrède, J.P. & Donnenberg, M.S. Enteropathogenic *Escherichia coli* EspF is targeted to mitochondria and is required to initiate the mitochondrial death pathway. *Cell. Microbiol.* **6**, 1097–1111 (2004).
54. Vallance, B.A., Deng, W., Jacobson, K. & Finlay, B.B. Host susceptibility to the attaching and effacing bacterial pathogen *Citrobacter rodentium*. *Infect. Immun.* **71**, 3443–3453 (2003).
55. Sham, H.P. *et al.* Attaching and effacing bacterial effector NleC suppresses epithelial inflammatory responses by inhibiting NF-κB and p38 mitogen-activated protein kinase activation. *Infect. Immun.* **79**, 3552–3562 (2011).
56. Choi, K.H. *et al.* A Tn7-based broad-range bacterial cloning and expression system. *Nat. Methods* **2**, 443–448 (2005).
57. Ferrières, L. *et al.* Silent mischief: bacteriophage Mu insertions contaminate products of *Escherichia coli* random mutagenesis performed using suicidal transposon delivery plasmids mobilized by broad-host-range RP4 conjugative machinery. *J. Bacteriol.* **192**, 6418–6427 (2010).
58. Ding, Y., Shen, S., Lino, A.C., Curotto de Lafaille, M.A. & Lafaille, J.J. β-catenin stabilization extends regulatory T cell survival and induces anergy in nonregulatory T cells. *Nat. Med.* **14**, 162–169 (2008).
59. Powrie, F., Carlino, J., Leach, M.W., Mauze, S. & Coffman, R.L. A critical role for transforming growth factor-β but not interleukin 4 in the suppression of T helper type 1-mediated colitis by $CD45RB^{low}$ $CD4^{+}$ T cells. *J. Exp. Med.* **183**, 2669–2674 (1996).